

Supporting Information

Hermosura et al. 10.1073/pnas.0808218105

SI Text

Genotyping: Specimens, PCR, Sequencing. The same set of samples described in an earlier study were used (1), except that control samples were limited to 22 because of sample depletion, instead of 23. Primer design, genomic DNA extraction, PCR, sequencing reactions, and alignments were conducted as described in that study (1). Primer sequences were designed based on the published human sequence for *TRPM2* (NC_000021.7) and available on request. Specimens were labeled simply with their numeric codes, and staff members who handled the samples and ran the reactions were kept blinded as to the diagnosis. Samples were sequenced in both directions, then aligned against the published *TRPM2* genomic and mRNA reference sequences (NC_000021.7 and NM_003307, respectively).

Computer Modeling and Structural Prediction of the S6 Transmembrane Motif of TRPM2 and TRPM2^{P1018L}. We used the HHpred remote homology-detection server (2) and identified two channel proteins with significant detection parameters (E value, 1.7×10^{-3} to 3.7×10^{-2} ; *P* value, 1.1×10^{-7} to 2.4×10^{-6} ; and score, 31.7–25.8, respectively) as potential structural templates for S6 of TRPM2 and TRPM2^{P1018L}. The candidates found were the K⁺ voltage-gated channel subfamily A member 2 protein from *Rattus norvegicus*, (Protein Data Bank code 2a79_B) and the K⁺ channel fragment KvAP from *Aeropyrum pernix* (Protein Data Bank code 1orq_C). We used the structure of 2a79_B to build the comparative models using the ESyPred3D homology modeling server (3). Geometry optimization and molecular rendering was performed with the software program DS ViewerPro (Accelrys). Validation of the global and regional quality of the model was made with the program Verify3D (4). The local stereochemical quality was assessed with the program Procheck (5).

Constructs, Mutagenesis, and Creation of Stable Cell Lines. Human TRPM2 WT cloning and establishment of stable inducible expression of the channel in HEK-293 T-Rex cells (Invitrogen) has been previously described (6). TRPM2^{P1018L} was generated by site-directed mutagenesis using the QuikChange kit (Stratagene) following the standard protocol. The predicted DNA sequence was verified by sequencing. Stable inducible expression of TRPM2^{P1018L} in HEK-293 cells was obtained according to the same protocol as for TRPM2 WT.

Western Blots and Surface Biotinylation Assays. HEK-293 cells (0.5 to 1×10^7) with doxycycline-inducible expression of the indicated channels were plated, and expression induced by adding doxycycline for 24 to 48 h. Anti-Flag (Sigma) immunoprecipitations were performed from lysates. Immunoprecipitated proteins were washed three times with lysis buffer, separated by SDS/PAGE using 6% polyacrylamide gels, transferred to a

PVDF membrane, and analyzed by anti-Flag. For surface labeling experiments, intact cells were incubated with biotin (Pierce). Residual biotinylation reagents were inactivated, and cells were lysed and then immunoprecipitated with anti-Flag. The anti-Flag immunoprecipitates were washed extensively and immunoblotted with streptavidin-HRP (Sigma) to detect cell surface-expressed proteins. The blots were then stripped and immunoblotted with anti-Flag to detect total TRPM2 expression.

Cell Culture. Cells stably expressing WT or P1018L TRPM2 were grown on glass coverslips at 37°C in DMEM plus 10% FBS, 5 μ g/ml blasticidin and 0.4 mg/ml Zeocin in the presence of 5% CO₂ and passaged twice a week. Cells were not used beyond 20 passages. Channel expression was induced by the addition of 1 μ g/ml doxycycline to the culture medium.

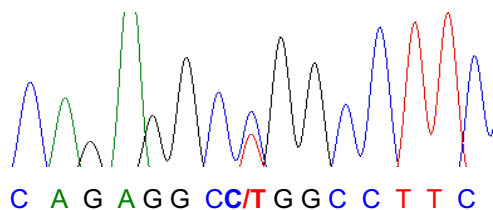
Fura-2 Ca²⁺ Experiments. Cytosolic [Ca²⁺]_i was monitored in a cuvette-based assay by detecting changes in Fura-2 fluorescence using the QM-6/2003 fluorometer (Photon Technology International). Standard labeling protocols were used. Briefly, cells were plated for 18 to 24 h before analysis and either left untreated or treated with 1 μ g/ml doxycycline in normal growth media. The cells were then loaded with Fura-2 (Molecular Probes) for 30 min at 37°C in loading buffer (135 mM NaCl, 5 mM KCl, 1 mM CaCl₂, 1 mM MgCl₂, 5.6 mM glucose, 10 mM Hepes, 0.1% BSA), washed, and measured by exposure every 2 sec to 340/380 nm excitation accompanied by monitoring 510 nm emission light for the period. L-BMAA (1 mM final) and H₂O₂ (10 and 100 μ M final)—both from Sigma—were added directly into the cuvette as indicated.

Electrophysiology. The cells were induced with doxycycline for 16 to 22 h. They were then placed in a standard bath solution of the following composition (mM): NaCl 140 to 145, KCl 2.8, Hepes-NaOH 10, CaCl₂ 1.5, MgCl₂ 1, glucose 10; osmolarity, 295 to 315 mOsm. The standard internal (pipette) solution contained (in mM): Cs- or K-glutamate 140 to 145, NaCl 8, Hepes-CsOH 10, MgCl₂ 2. In cases in which buffered [Ca²⁺]_i was needed, appropriate amounts of 1 M stock Ca²⁺ solution, calculated using MaxChelator (<http://www.stanford.edu/~cpaton/maxc.html>), and 10 mM Cs- or K-EGTA were added. To obtain 1 μ M [Ca²⁺]_i, 0.886 mM CaCl₂ and 1 mM Cs- or K-EGTA were used (7). The pH was adjusted to 7.4 and osmolarity measured (normally 300–315 mOsm). Ca²⁺ or Mg²⁺ was not added to the bath or internal solution as required (for specific experiments). When [Ca²⁺]_o was varied, the appropriate amount of 1 M stock solution was added to a 0-Ca²⁺ bath solution. ADPR and L-BMAA (Sigma) were prepared in 100 mM frozen aliquots and used as needed. Patch-clamp experiments were performed in the tight-seal, whole-cell configuration at RT (23°C–25°C), unless otherwise specified, and conducted as previously described (1).

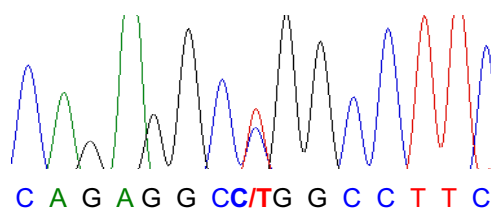
1. Hermosura MC, et al. (2005) A TRPM7 variant shows altered sensitivity to magnesium that may contribute to the pathogenesis of two Guamanian neurodegenerative disorders. *Proc Natl Acad Sci USA* 102:11510–11515.
2. Söding J, Biegert A, Lupas AN (2005) The HHpred interactive server for protein homology detection and structure prediction. *Nucleic Acids Res* 33:W244–W248.
3. Lambert C, Leonard N, De Bolle X, Depiereux E (2002) ESyPred3D: prediction of proteins 3D structures. *Bioinformatics* 18:1250–1256.
4. Luthy R, Bowie JU, Eisenberg D (1992) Assessment of protein models with three dimensional profiles. *Nature* 356:83–85.

5. Laskowski RA, MacArthur MW, Moss DS, Thornton JM (1993) PROCHECK: a program to check the stereochemical quality of protein structures. *J Appl Cryst* 26:283–291.
6. Perraud AL, et al. (2001) ADP-ribose gating of the calcium-permeable LTRPC2 channel revealed by Nudix motif homology. *Nature* 411:595–599.
7. Heiner I, et al. (2006) Endogenous ADP-ribose enables calcium-regulated cation currents through TRPM2 channels in neutrophil granulocytes. *Biochem J* 398:225–232.

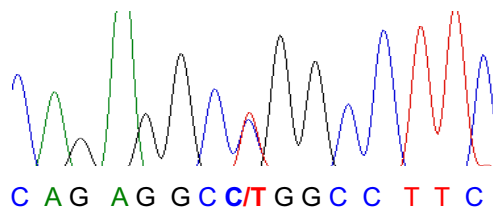
ALS-G (#5)



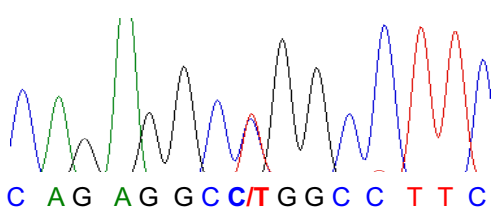
PDC (#25)



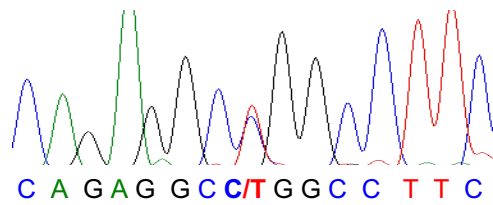
ALS-G (#29)



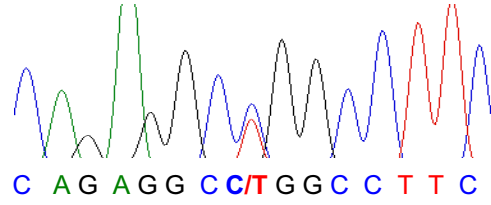
PDC (#45)



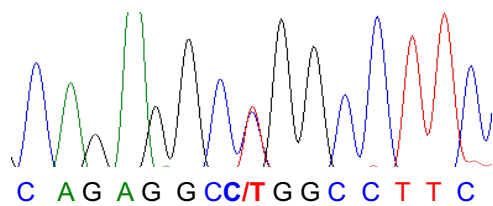
ALS-G (#27)



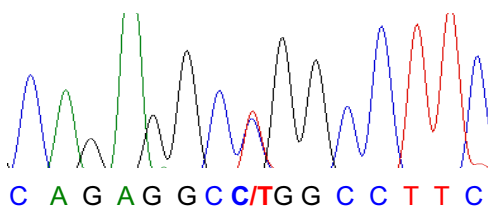
Control-HRT (#2)



ALS-G (#43)



Control-HRT (#41)



Control-Tumor (#32)

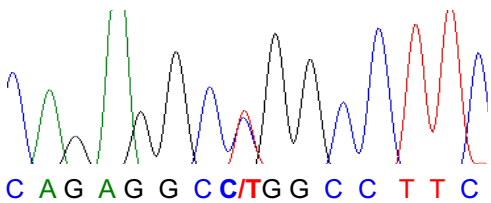


Fig. S1. Sequence chromatograms of all samples heterozygous for *TRPM2*^{P1018L}.

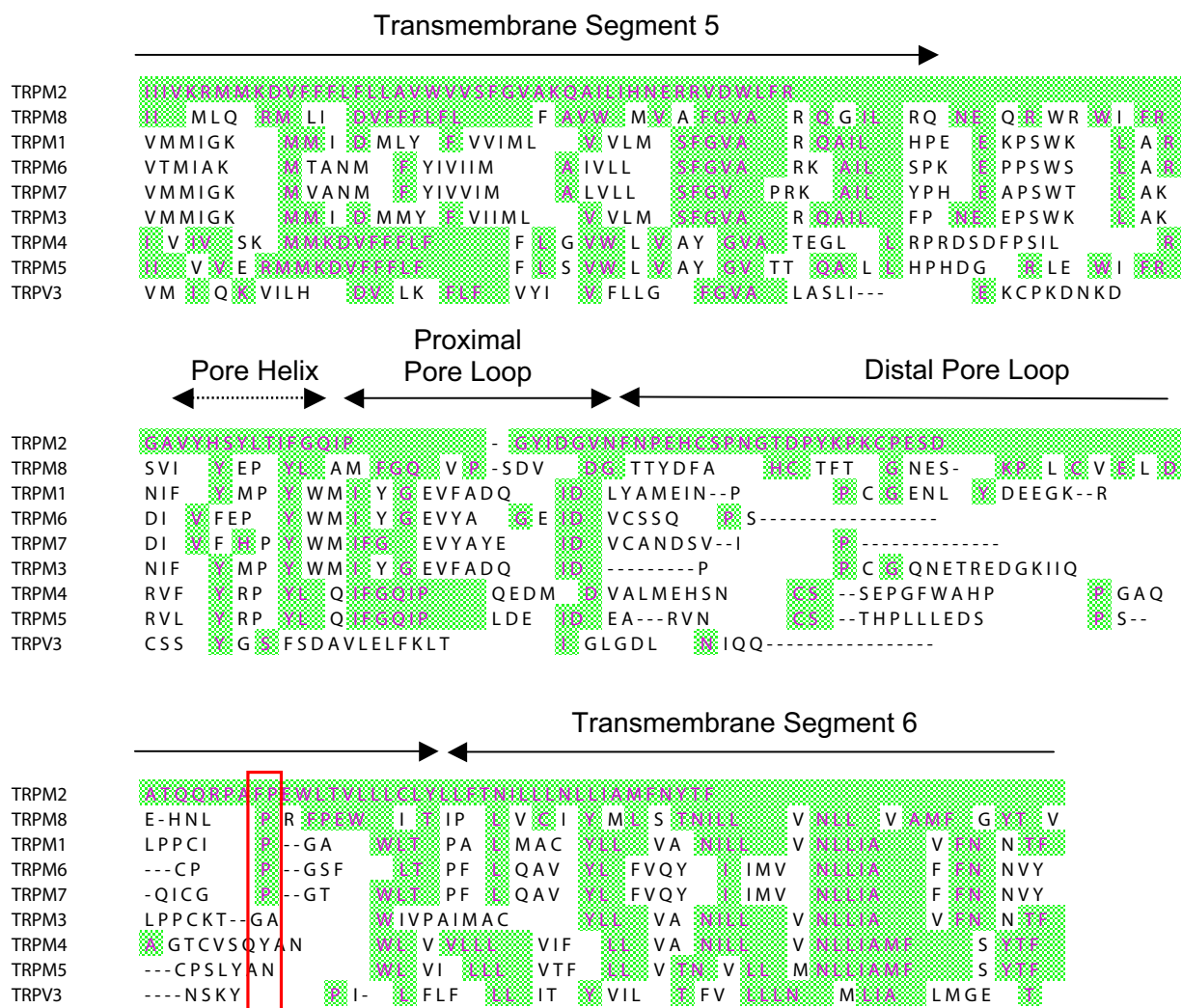


Fig. S2. Clustal W alignment of human TRPM and TRPV3 protein sequences. Among all known human TRP channels, only TRPV3 aligned with any significance in the region of interest (between S5, pore, and S6). Residues highlighted in green are identical to the ones in TRPM2; Pro¹⁰¹⁸ and homologues are boxed in red. The predicted subregions and segments were marked as shown in Mederos y Schnitzler *et al.* (ref. 20 in main text). National Center for Biotechnology Information accession numbers are: TRPM2, NP_003298.1; TRPM8, NP_076985.4; TRPM1, NP_002411.3; TRPM6, NP_060132.3; TRPM7, NP_060142.3; TRPM3, NP_001007472.2; TRPM4, NP_060106.2; TRPM5, NP_055370.1; TRPV3, NP_659505.1.

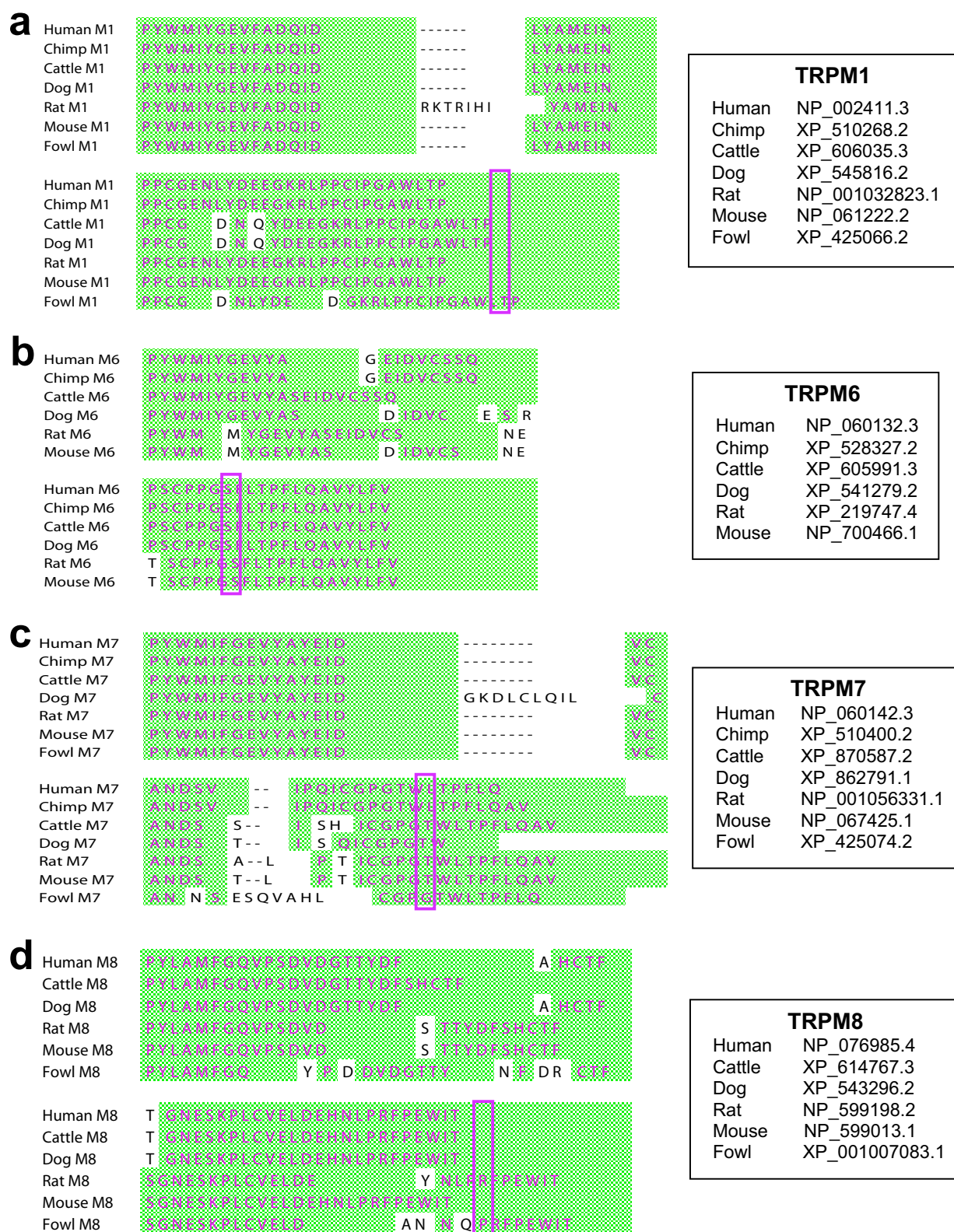


Fig. S3. Multiple alignments of sequences in the putative distal pore loop and part of S6. The homologues of Pro¹⁰¹⁸ in TRPM1 (a), TRPM6 (b), TRPM7 (c), and TRPM8(d) are evolutionary conserved (boxed). Residues highlighted in green are 100% conserved in the species shown. The National Center for Biotechnology Information accession number for each channel is listed (Right).

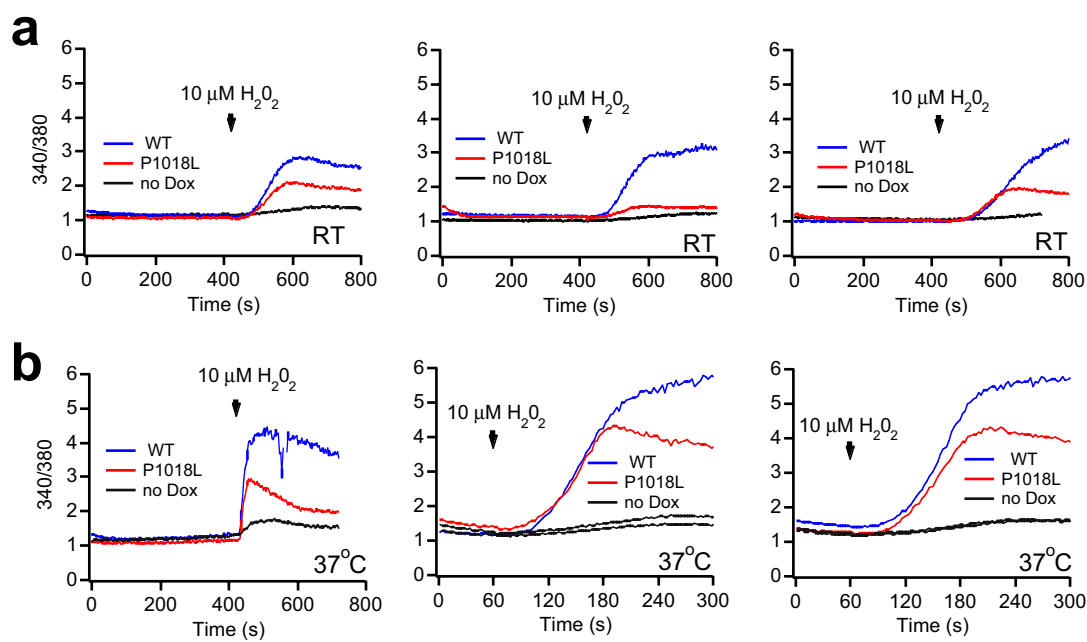
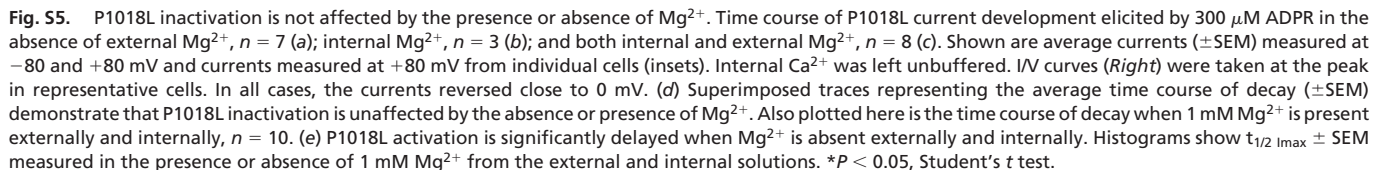


Fig. S4. The Ca^{2+} increase elicited by 10 μM H_2O_2 is consistently attenuated in P1018L cells. Three independent experiments were each performed at room temperature (RT) (a) and 37°C (b). In these examples, the average Ca^{2+} increases evoked by 10 μM H_2O_2 at 37°C in WT were 3.9 ± 0.5 (SEM) in ratio of fluorescence units (RFU) and 2.6 ± 0.5 RFU in P1018L, a 1.5-fold difference. At RT, the average Ca^{2+} increases in WT were 2.0 ± 0.5 RFU and 0.7 ± 0.3 RFU in P1018L, a 2.7-fold difference.



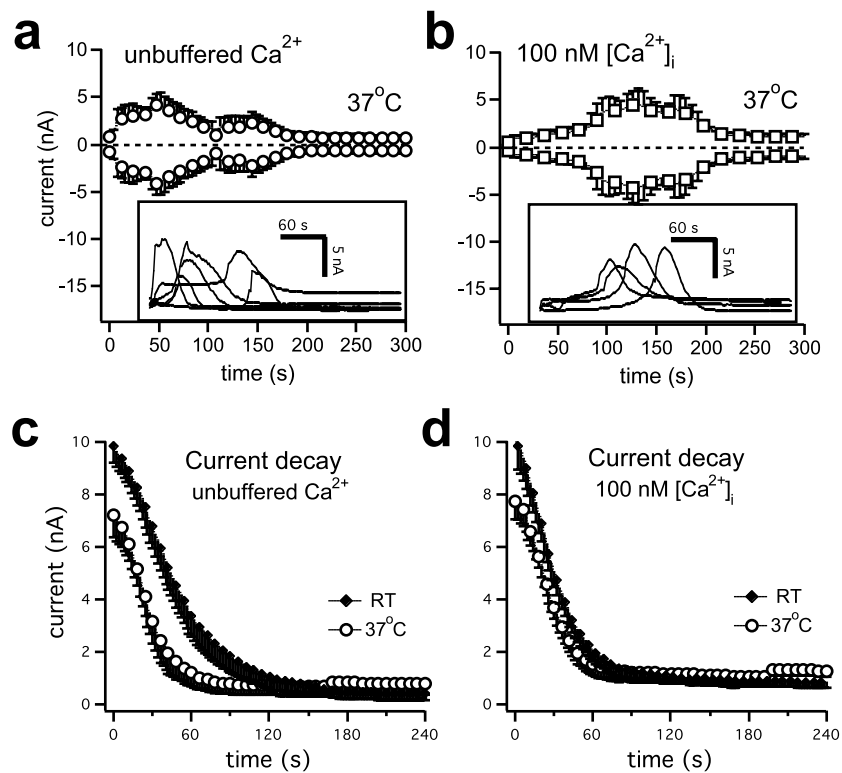
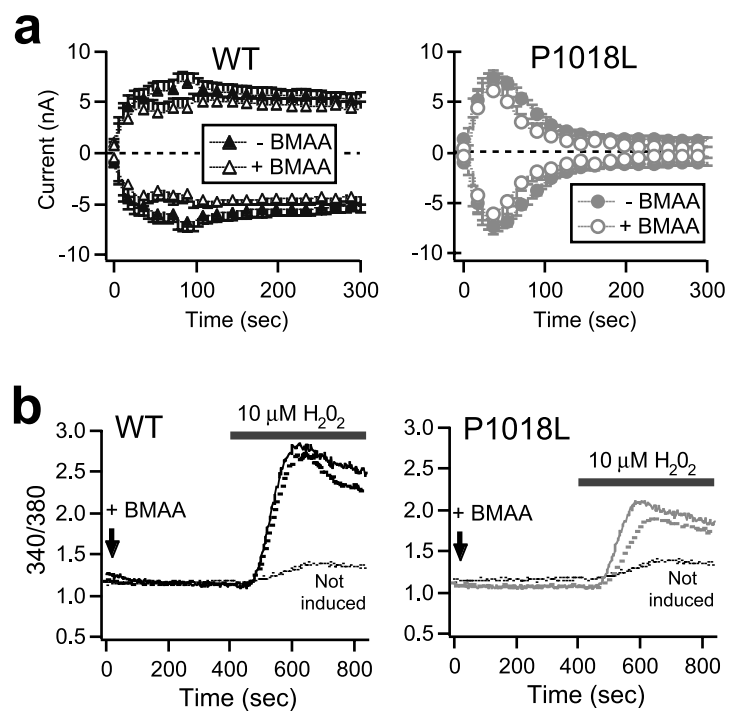


Fig. S6. P1018L inactivation proceeds similarly at 37°C and RT. Time course of P1018L current development elicited by 300 μM ADPR at 37°C in unbuffered $[\text{Ca}^{2+}]_i$, $n = 6$ (a); and 100 nM $[\text{Ca}^{2+}]_i$, $n = 4$ (b). Shown are average currents ($\pm\text{SEM}$) measured at -80 and $+80$ mV and currents measured at $+80$ mV from individual cells (insets). The time course of decay at 37°C is not significantly different from the time course of decay at RT, in the presence of unbuffered $[\text{Ca}^{2+}]_i$ (c), or 100 nM $[\text{Ca}^{2+}]_i$ (d). (c) The $t_{1/2 \text{ decay}}$ values are 29.2 ± 9.3 (mean \pm SD) at 37°C and 49.5 ± 28.3 at room temperature (RT). These are not significantly different ($P > 0.05$, Student t test).



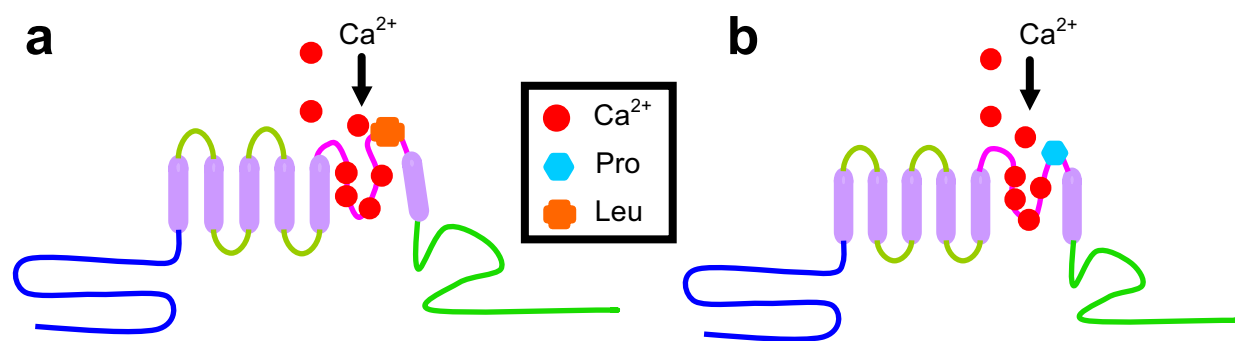


Fig. S8. Tentative model for P1018L inactivation. (a) In the presence of Leu¹⁰¹⁸, a slightly bigger loop is formed at the junction between the distal end of the pore and the extracellular end of S6. The resulting relaxation of structural constraints favor conformational changes that lead to occlusion of the pore when Ca^{2+} ions are bound to binding sites in the pore domain. (b) Pro¹⁰¹⁸ maintains structural integrity of the outer pore region under the same conditions.